Effectiveness of Capillary Barrier and Vegetative Slope Covers in Maintaining Soil Suction

H. Rahardjo, S. Krisnanto, E.C. Leong

Abstract. Capillary barrier and vegetative slope covers can be used to improve slope stability during rainfall by maintaining matric suction in the slope. A study was performed to investigate the effectiveness of capillary barrier system (CBS) and vegetative slope covers (Orange Jasmine and Vetiver grass) in maintaining soil suction. Performance of slopes with and without slope covers was investigated using field instrumentations and numerical analyses. Laboratory tests were performed to measure hydraulic and shear strength properties of the soil, the soils with Orange Jasmine and Vetiver grass root, and CBS materials. Numerical analyses were performed to investigate the variation of pore-water pressure profiles at a selected location and factor of safety during low, high, and maximum rainfall intensities. Pore-water pressures measured in the field were used to calibrate the numerical models. Laboratory test results showed that the presence of root increased the shear strength of soil. Numerical analyses and field monitoring results showed that the slope with covers can maintain negative pore-water pressure better than the original slope. Performance of Orange Jasmine, Vetiver grass, and CBS in maintaining matric suction in the slope is essentially similar during low, high, and maximum rainfall intensities.
Keywords: slope covers, stability, soil suction, infiltration, instrumentation.

1. Introduction

Residual soils commonly exist in many tropical areas. These soils are often in the unsaturated condition with negative pore-water pressure (matric suction). The presence of matric suction increases shear strength of the soil. Therefore, the presence of matric suction is a favorable condition for slope stability. However, rainfall infiltration into slope will increase pore-water pressure or decrease matric suction in soil, resulting in a decrease in shear strength of the soil. The decrease of shear strength causes the slope to become more prone to failure that is commonly referred to as rainfall-induced slope failure (Pitts 1985; Tan *et al.*, 1987; Brand 1992; Gasmo *et al.*, 2000; Tsaparas *et al.*, 2002).

Capillary barrier system (CBS) is a two-layer system of soil cover that is designed based on unsaturated soil mechanics principles. CBS consists of a fine-grained soil layer placed on top of a coarse-grained soil layer. The contrast in soil-water characteristic curve (SWCC) and permeability function between these two layers is utilized to create a barrier to minimize water infiltration into the underlying soil.

Capillary barrier system (CBS) can be used to mitigate rainfall-induced slope failures (Ross 1990; Steenhuis *et al.*, 1991; Morel-Seytoux 1993, 1994; Stormont 1996; Morris & Stormont 1997a, 1997b; Khire *et al.*, 2000; Tami *et al.*, 2004a, 2004b; Yang *et al.*, 2004b; Krisdani *et al.*, 2008). CBS consists of two different soil layers with a significant difference in their soil-water characteristic curves (SWCC) and permeability functions that serves to minimize water seepage into the underlying layers.

Besides CBS, vegetative cover can also be used to mitigate rainfall-induced slope failure (*e.g.* Grimshaw 1994; Thruong & Gawander 1996; World Bank 1995; National Research Council 1993). The presence of root can increase shear strength of soil (Styczen & Morgan 1995). Orange Jasmine, *Murraya exotica L.*, and Vetiver grass, *Chrysopogon zizaniodes*, are evergreen vegetations that can be planted in a tropical area like Singapore. They can adapt to variation in weather conditions and require minimum maintenance. Because of these characteristics, Orange Jasmine and Vetiver grass are potential vegetations to be used as soil covers to overcome rainfall-induced failure problems in the tropics.

Each slope cover may perform differently in maintaining matric suction. In addition, the performance of slope cover may differ under different rainfall intensities. Therefore, there is a need to investigate the effectiveness of capillary barrier and vegetative slope covers in maintaining soil suction.

The objective of this study is to compare the performance of Orange Jasmine and Vetiver grass slope covers and CBS in maintaining matric suction through field measurements and numerical analyses. The effect of Orange Jasmine and Vetiver grass roots on soil shear strength is also investigated through laboratory tests.

H. Rahardjo, Professor, School of Civil & Environmental Engineering, Nanyang Technological University, Blk N1, #1B-36, 50 Nanyang Avenue, 639798, Singapore. e-mail: chrahardjo@ntu.edu.sg.
S. Krisnanto, Lecturer, Geotechnical Engineering Research Division, Faculty of Civil & Environmental Engineering, Bandung Institute of Technology, Soil Mechanics Laboratory, CIBE Building, Jalan Ganesha No. 10, Bandung 40132, Indonesia. e-mail: sugeng.krisnanto@ftsl.itb.ac.id.
E.C. Leong, Associate Professor, School of Civil & Environmental Engineering, Nanyang Technological University, Blk N1, #1C-80, 50 Nanyang Avenue, 639798, Singapore. e-mail: cecleong@ntu.edu.sg.
Invited Article, no discussion.

2. Site Overview

The geology of Singapore consists of Old Alluvium in the eastern and northeastern regions, the sedimentary Jurong Formation in the western region, and Bukit Timah Granite in the center and northwestern regions.

A slope consists of soil from the Old Alluvium was selected for this study. The slope has a height of 8.21 m, a length of 22.55 m, and a slope angle of 20°. The slope was divided into three sections: the first section was the original slope covered with cow grass, the second section was covered with Orange Jasmine, the third section was covered with Vetiver grass, and the fourth section was covered with CBS. Layout of the slope is shown in Fig. 1. Based on soil investigation and laboratory tests, it was found that the slope consists of two layers of residual soils, named as layer 1 and layer 2. A relatively thin sub layer with saturated permeability lower than those of layers 1 and 2 was found within layer 1. Schematic diagrams of each section of the slope are shown in Fig. 2.

3. Design of Slopes and Field Instrumentation

The original slope was covered by cow grass surrounded by trench (Fig. 1). The original slope was instrumented with three Casagrande piezometers and three tensiometers (Fig. 2(a)). The piezometers were installed at near the crest, middle and near the toe of the slope. The tensiometers were labelled as TA3, TB3, and TD3 with a spacing of 0.5 m and insertion depths of 0.67 m, 1.29 m, and 1.84 m, respectively (Fig. 2(a)). Polyvinyl chloride (PVC) casings were installed at the locations of tensiometers and piezometers for installing the instruments.

Schematic diagram of the slope covered with Orange Jasmine and Vetiver grass is shown in Fig. 2(b). Orange Jasmine and Vetiver grass were planted in June and September 2009, respectively. In this study, only direct rainfall infiltration onto the covered slope had to be observed. Therefore, the lateral water flow from the surrounding soil into the vegetated area must be prevented. To achieve this condition, the vegetated areas were surrounded by a trench and impermeable metal sheets that were installed to 600 mm depth from the slope surface (Fig. 2(b)). PVC casings for tensiometers were installed at the planned locations of tensiometers. Before planting the vegetations, erosion blanket was laid on the slope surface to protect the slope within the study area from erosion during rainfall. Orange Jasmine was planted with lateral and down slope spacing of 450 mm whereas Vetiver grass was planted with lateral spacing of 250 mm and down slope spacing of 450 mm to avoid overlapping roots between adjacent vegetations. In the slope with Orange Jasmine, three tensiometers were installed. The installed tensiometers were labelled as TE4, TA4, and TB4 with a spacing of 0.5 m and insertion depths of 0.4 m, 0.66 m, and 1.21 m, respectively. In the slope with Vetiver grass, three tensiometers were also installed. The installed tensiometers were labelled as TE5, TA5, and TB5 with a spacing of 0.5 m and insertion depths of 0.4 m, 0.67 m, and 1.24 m, respectively.

Schematic diagram of the slope covered with CBS is shown in Fig. 2(c). To construct the CBS, the slope surface was excavated to 540 mm depth below the slope surface. Similar to the slope sections with vegetations, the CBS area was also surrounded by trench and impermeable metal sheets. A 6.5 mm thick layer of a geosynthetic drainage system (Secudrain) was used as a separator between the fine-grained layer and the original soil. J-pins of 75 cm and 115 cm in length penetrating 54 cm and 75 cm into the ground, respectively, were installed. PVC casings for tensiometers were installed at the planned locations of tensiometers. Geocells were laid on top of the secudrain for con-

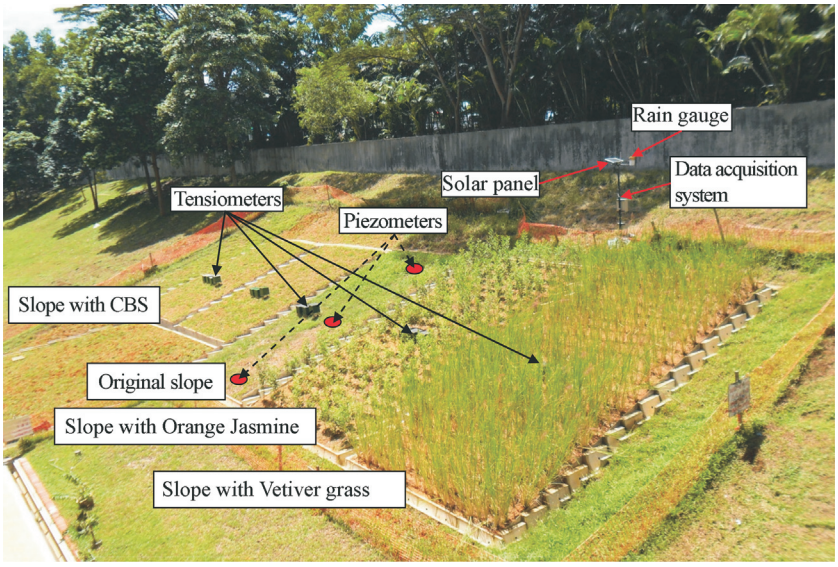

Figure 1 - Layout of the investigated slope.

taining the coarse-grained layer secured by the 75 cm long J-pins. Recycled concrete aggregate (RCA) as the coarse-grained layer was backfilled into the geocells and compacted to a relative density (D_r) between 70%-90% or to the required dry density (ρ_d) of 1.80 g/cm^3. A nonwoven geotextile TS 80 (TenCate 2011) was used in the capillary barrier as a separator between the coarse- and fine-grained layers. Geocells for containing the fine-grained layer were laid on top of the nonwoven geotextile secured by the 115 cm length J-pins. Fine sand for the fine-grained layer was backfilled into the geocells and compacted to a relative density (D_r) between 70%-90% or to the required dry density (ρ_d) of 1.65 g/cm^3. Perforated PVC pipes (diameter 15 mm) wrapped with the nonwoven geotextile TS 20 (TenCate

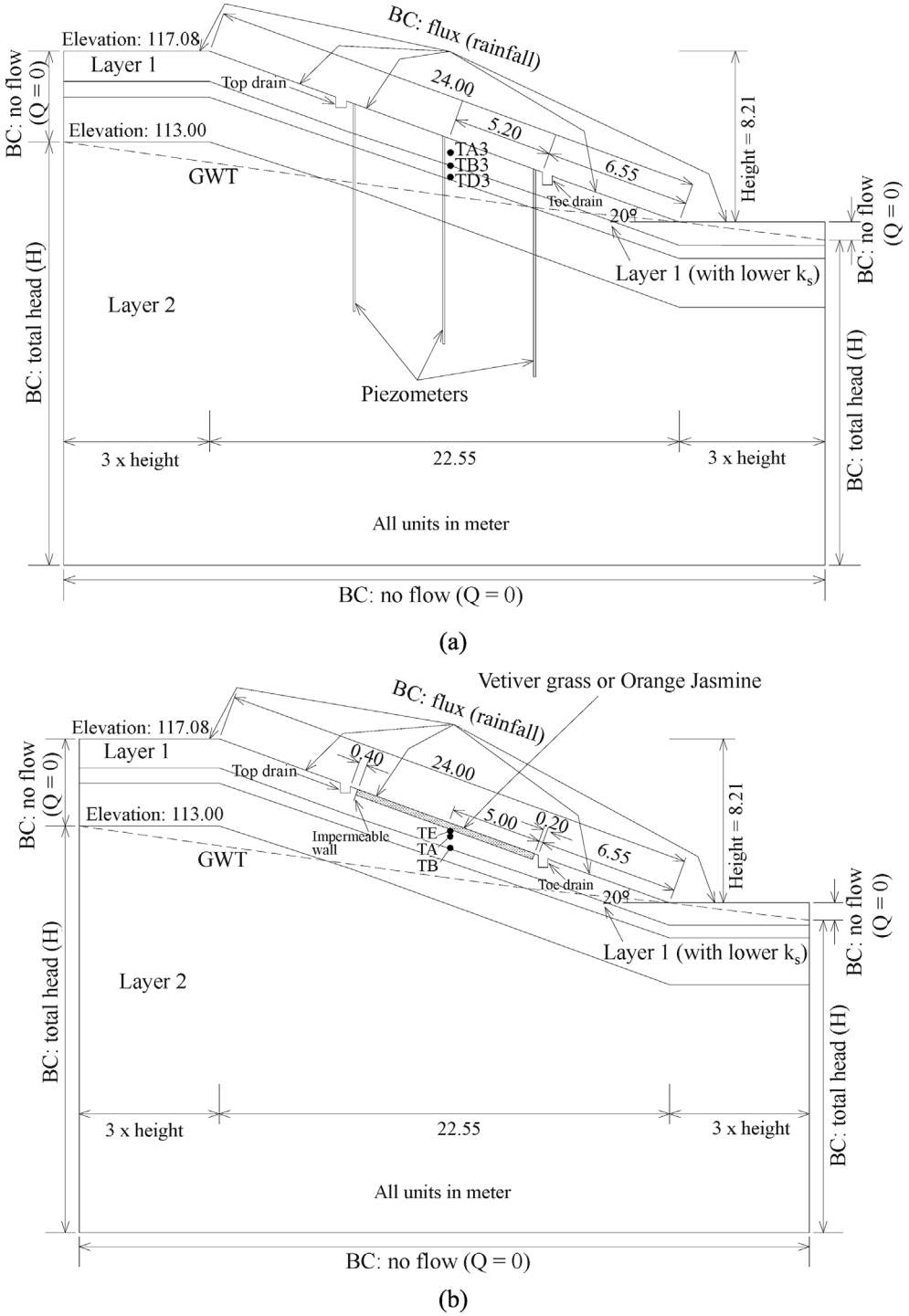

Figure 2 - Schematic diagram of slope with vegetation and CBS: (a) original slope, (b) slope with Orange Jasmine and Vetiver grass.

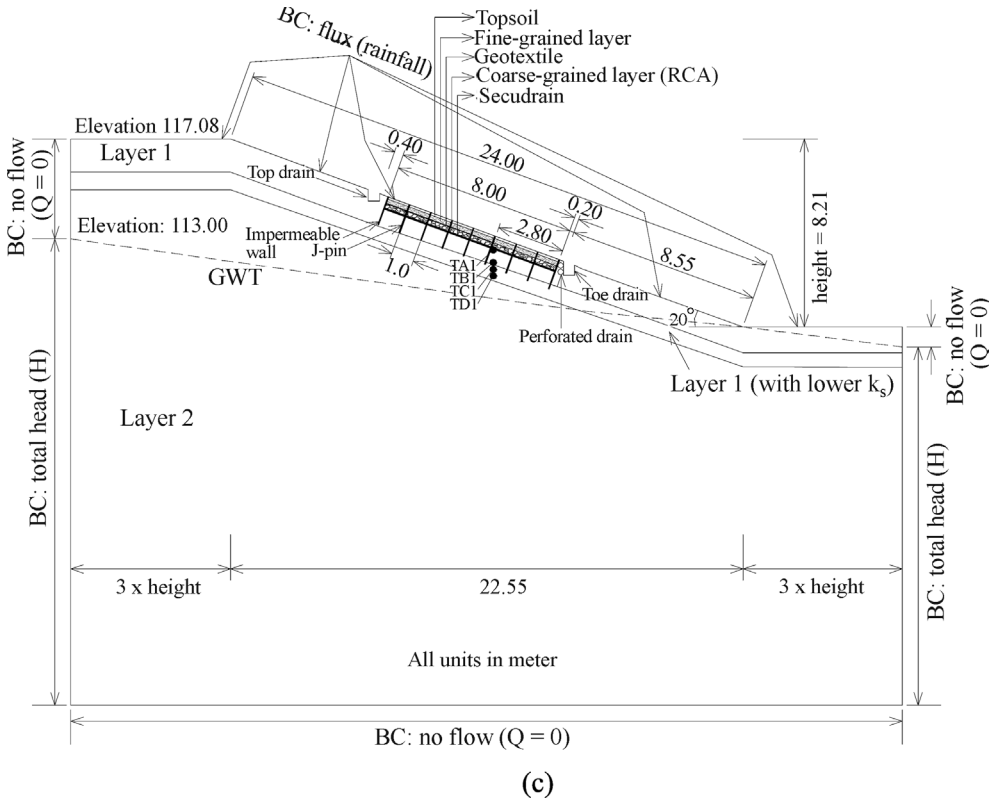

(c)

Figure 2 (cont) - (c) slope with CBS with recycled concrete as the coarse-grained layer.

2011) were installed at the toe of the slope for collecting water that flowed through the coarse- and the fine-grained layers to the toe of the slope. The erosion control blanket mat was placed below the top soil to prevent the erosion of fine-grained soil during heavy rainfall. The slope was then backfilled and compacted to the slope surface with top soil. In the slope with CBS, four tensiometers were installed. The installed tensiometers were labelled as TA1, TB1, TC1, and TD1 with a spacing of 0.5 m and insertion depths of 0.63, 1.18, 1.48, and 1.76 m, respectively (Fig. 2(c)).

A tipping bucket rain gauge was used to determine the amount of rainfall at the site (Fig. 1). A photovoltaic power supply system consisting of one module of solar panel and several reserve batteries was installed on the crest of the slope (Fig. 1). The tensiometers, piezometers, and rain gauge were connected to the same power supply and data logger to obtain the readings in real time which can be accessed on-line.

4. Laboratory Test and Soil Properties

Laboratory tests were carried out to determine saturated and unsaturated properties of layer 1, layer 2, soil with Orange Jasmine roots, soil with Vetiver grass roots, fine- and coarse-grained materials of the CBS. Index and engineering properties tests were carried out to obtain index properties, soil-water characteristic curve (SWCC), saturated and unsaturated permeability, and shear strength of the soils. The basic soil properties are summarized in Tables 1 to 3.

Table 1 - Basic properties of the soils without vegetation.

Description	Soil		
	Layer 1	Layer 1 (with lower k_s)	Layer 2
USCS	SP	SP	SP
Specific gravity, G_s	2.66	2.66	2.61
Water content, w (%)	21.1	16.8	25.8
Saturated coefficient of permeability, k_s (m/s)	8.7×10^{-8}	6.4×10^{-10}	5.0×10^{-8}
Organic content at 440 °C (%)	0	0	0
Organic content at 750 °C (%)	0	0	0

Table 2 - Basic properties of the soils with vegetation.

Description	Soil with Orange Jasmine Root			Soil with Vetiver Grass Root		
	29 Jul 2010	18 Nov 2010	28 Feb 2011	29 Jul 2010	18 Nov 2010	28 Feb 2011
USCS	SP	SP	SP	SP	SP	SP
Specific gravity, G_s	2.64	2.71	2.71	2.32	2.65	2.64
Water content, w (%)	18.0	17.3	22.6	23.4	23.4	17.2
Saturated coefficient of permeability, k_s (m/s)	5.5×10^{-8}	1.0×10^{-7}	2.4×10^{-8}	7.1×10^{-8}	5.0×10^{-8}	3.9×10^{-8}
Organic content at 440 °C (%)	1.1	3.1	2.9	1.2	2.1	5.4
Organic content at 750 °C (%)	3.9	5.1	6.1	1.9	4.4	9.2

Table 3 - Basic properties of CBS.

Description	Fine-grained layer	Coarse-grained layer (RCA)
USCS	SP	GP
Specific gravity, G_s	2.65	2.66
Gravel content (>4.75 mm; %)	0	100
Sand (%)	100	0
Fines (<0.075 mm; %)	0	0
Grain-size distribution:		
D_{60} (mm)	0.52	10.6
D_{30} (mm)	0.32	10.3
D_{10} (mm)	0.20	9.5
Coefficient of uniformity, C_u	2.60	1.12
Coefficient of curvature, C_c	0.98	1.05
Dry density, ρ_d (g/cm^3)	1.58	1.53
Void ratio, e	0.70	0.66
Saturated coefficient of permeability, k_s (m/s)	2.7×10^{-4}	7.5×10^{-3}

The SWCCs were determined by combining the results from Tempe cell tests (for matric suction up to 100 kPa) and pressure plate tests (for matric suction up to 1500 kPa). SWCCs were measured for both drying and wetting processes. The measured SWCCs were best-fitted using the Fredlund & Xing (1994) equation with the correction factor taken as 1 as suggested by Leong & Rahardjo (1997). SWCCs were obtained for both drying and wetting for several specimens of soil with vegetation. However, for some soil specimens, only drying SWCC was obtained. In the absence of wetting SWCC data, the wetting SWCC was predicted from the drying SWCC. The scaling method (Pham *et al.*, 2005) was used for estimating the wetting SWCC from the drying SWCC. The SWCCs of the soils used in this study are shown in Fig. 3 whereas the fitting parameters are shown in Tables 4 to 6.

Table 4 - Hydraulic properties of of the soils without vegetation.

Description	Symbol (unit)	Soil	
		Layer 1	Layer 2
Drying curve			
Saturated volumetric water content	θ_s	0.25	0.42
Air-entry value	Ψ_a (kPa)	1	12
Residual matric suction	Ψ_r (kPa)	9	600
Residual volumetric water content	θ_r	0.11	0.34
Fredlund & Xing (1994)	a (kPa)	1.55	16.6
Fitting parameters	n	4.42	1.02
	m	0.31	0.19
Wetting curve			
Water-entry value	Ψ_w (kPa)	30	600
Volumetric water content at Ψ_w	θ_w	0.1	0.33
Fredlund & Xing (1994)	a (kPa)	3.41	7.47
Fitting parameters	n	2.20	1.41
	m	0.28	0.09

The saturated permeability for layer 1, layer 2, soil with Orange Jasmine, soil with Vetiver grass, fine- and coarse-grained materials of the CBS are shown in Tables 1 to 3. Permeability functions were estimated using the statistical method (Fredlund & Rahardjo 1993) by utilizing SWCC and saturated permeability data. Permeability functions of the soils used in this study are shown in Fig. 4.

It can be observed from Fig. 3 and Table 5 that the saturated water content and the air-entry value (AEV) increased as time of observation increased. This occurred for soils with Vetiver grass (Fig. 3a and Table 5) as well as soils with Orange Jasmine (Fig. 3b and Table 5). Table 2 shows that as time of observation increased, organic content also increased. The increase in organic content indicated that there was an increase in the volume of roots in

Table 5 - Hydraulic properties of the soils with vegetations.

Description	Symbol (unit)	Soil with Orange Jasmine root			Soil with Vetiver Grass root		
		29 Jul 2010	18 Nov 2010	28 Feb 2011	29 Jul 2010	18 Nov 2010	28 Feb 2011
Drying curve							
Saturated volumetric water content	θ_s	0.32	0.37	0.41	0.27	0.28	0.30
Air-entry value	Ψ_a (kPa)	1.3	2.0	4.0	2.2	4.1	4.6
Residual matric suction	Ψ_r (kPa)	553	734	859	7118	7716	9684
Residual volumetric water content	θ_r	0.14	0.16	0.17	0.18	0.19	0.19
Fredlund & Xing (1994)	*a* (kPa)	5.61	7.90	13.05	8.43	14.00	17.20
Fitting parameters	*n*	0.98	1.05	1.20	1.01	1.11	1.04
	m	0.55	0.53	0.51	0.21	0.21	0.24
Wetting curve							
Water-entry value	Ψ_w (kPa)	770	1263	1511	8796	24364	55064
Volumetric water content at Ψ_w	θ_w	0.12	0.15	0.16	0.18	0.17	0.18
Fredlund & Xing (1994)	*a* (kPa)	3.52	2.50	4.13	3.41	4.43	5.44
Fitting parameters	*n*	0.81	0.70	0.79	2.20	0.80	0.70
	m	0.53	0.53	0.51	0.28	0.21	0.24

Table 6 - Hydraulic properties of CBS.

Description	Symbol (unit)	Soil		Secudrain
		Fine-grained layer	RCA	
Drying curve				
Saturated volumetric water content	θ_s	0.41	0.47	0.69
Air-entry value	Ψ_a (kPa)	1.4	0.03	0.4
Residual matric suction	Ψ_r (kPa)	0.07	0.20	1.8
Residual volumetric water content	θ_r	0.04	0.13	0
Fredlund & Xing (1994)	*a* (kPa)	1.94	0.05	4.45
Fitting parameters	*n*	6.3	7.97	2.17
	m	0.87	0.47	70.69
Wetting curve				
Water-entry value	Ψ_w (kPa)	3.5	0.20	0.22
Volumetric water content at Ψ_w	θ_w	0.01	0.11	0
Fredlund & Xing (1994)	*a* (kPa)	1.81	0.56	0.18
Fitting parameters	*n*	3.19	0.21	5.1
	m	3.74	0.80	5.25

soil. Therefore, it can be inferred that the growth of root resulted in an increase in the saturated water content and AEV of the soil.

Saturated and unsaturated consolidated drained (CD) triaxial tests (Fredlund and Rahardjo, 1993) were performed to obtain shear strength parameters of soils without vegetation and soils with vegetations. Shear strength properties are shown in Table 7. Shear strength failure envelopes of the soil with Orange Jasmine roots and Vetiver grass roots are shown in Figs. 5 and 6, respectively. The

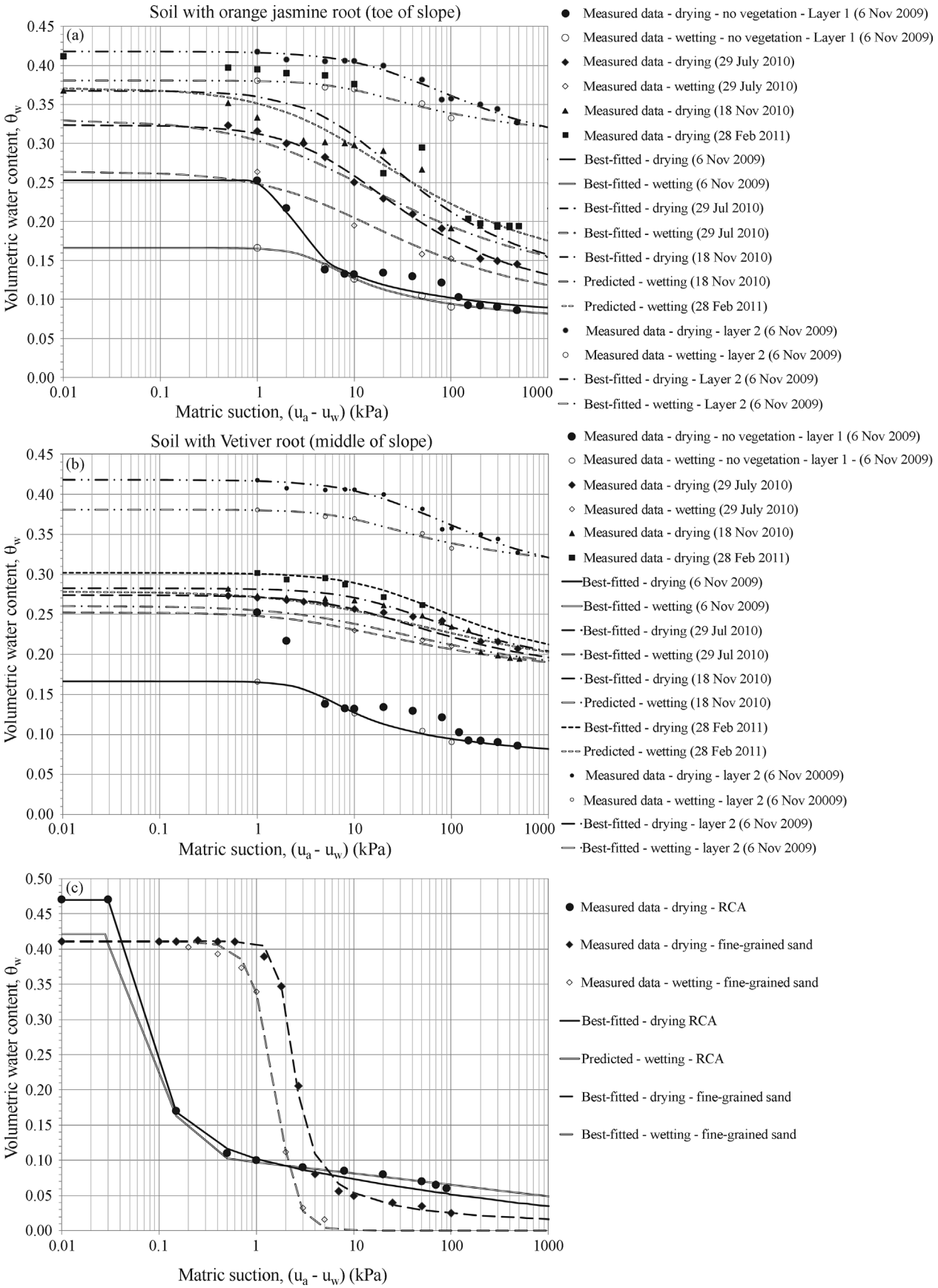

Figure 3 - SWCCs of the soils used in the study. (a) Soil with Orange Jasmine roots.

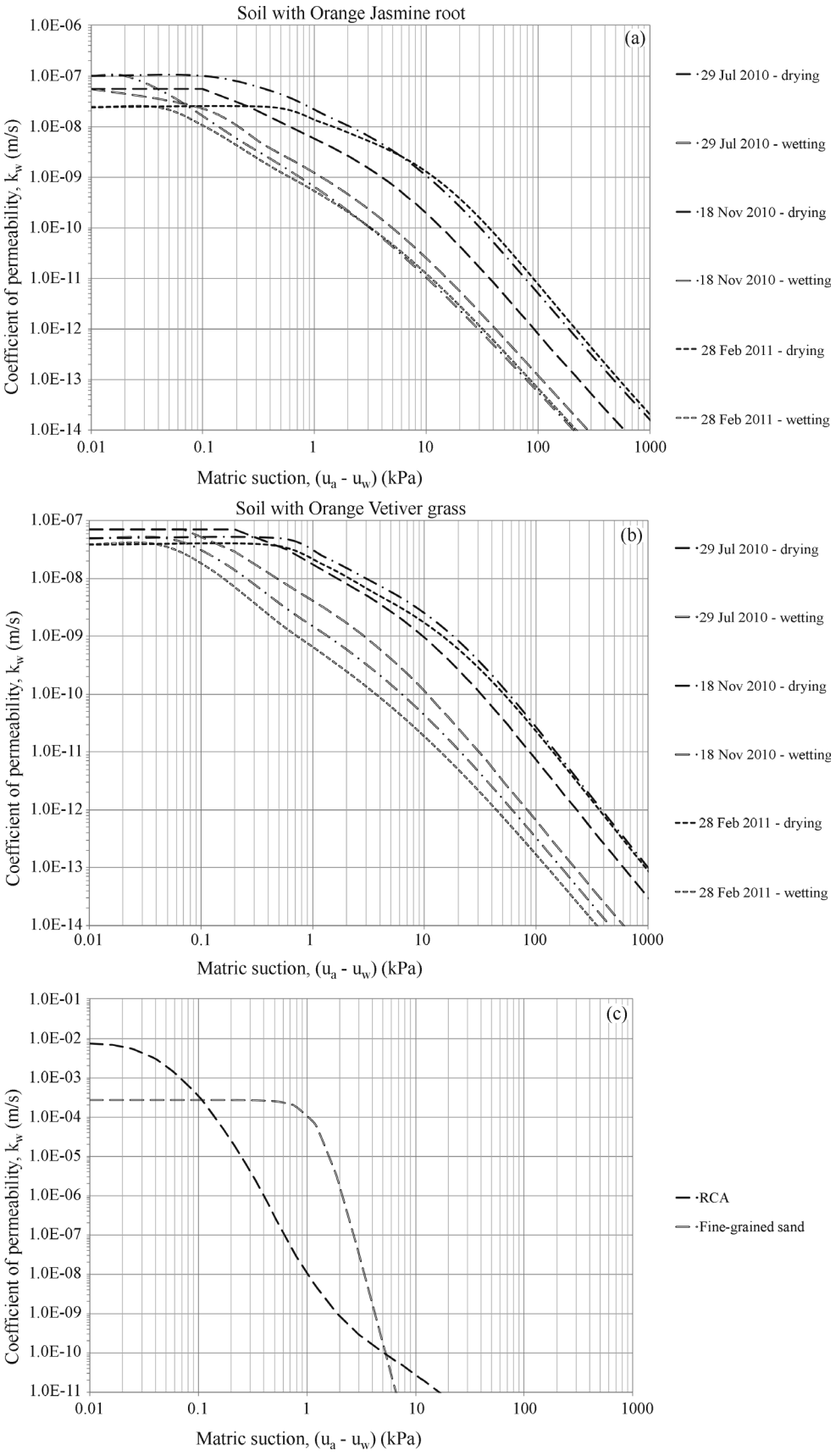

Figure 4 - Permeability functions of the soils used in the study. (a) Soil with Orange Jasmine roots. (b) Soil with Vetiver Grass roots. (c) CBS with RCA as the coarse-grained layer.

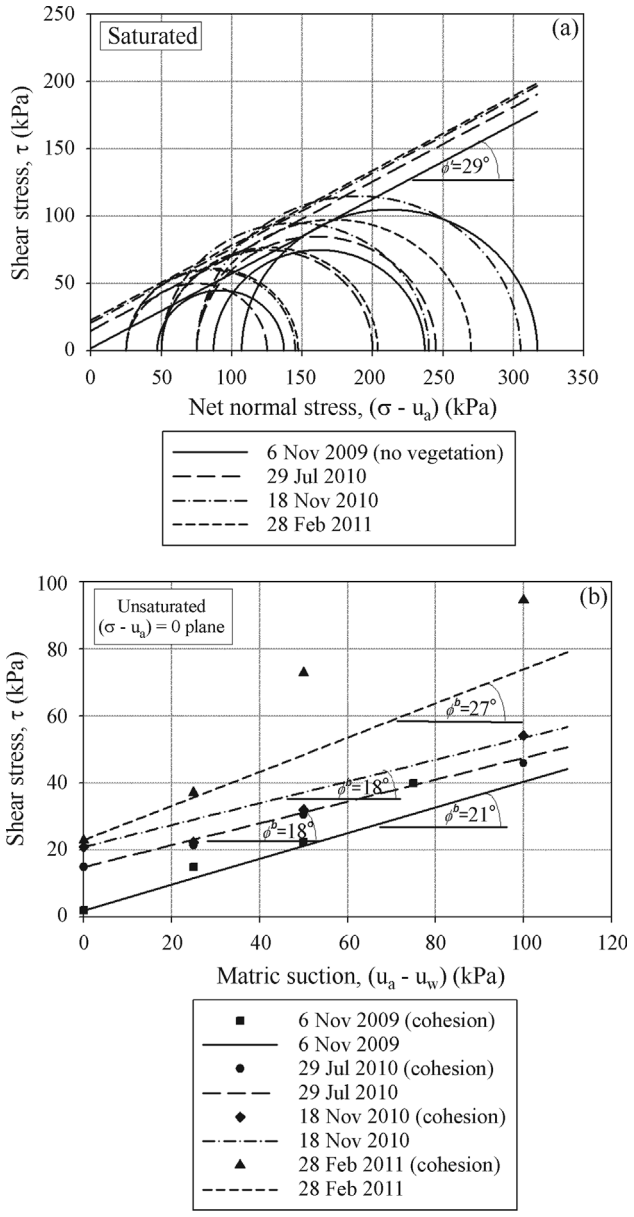

Figure 5 - Mohr-Coulomb failure envelopes of original soil and soil with Orange Jasmine roots: (a) at zero matric suction, (b) at matric suctions greater than zero and on $(\sigma - u_a) = 0$ plane.

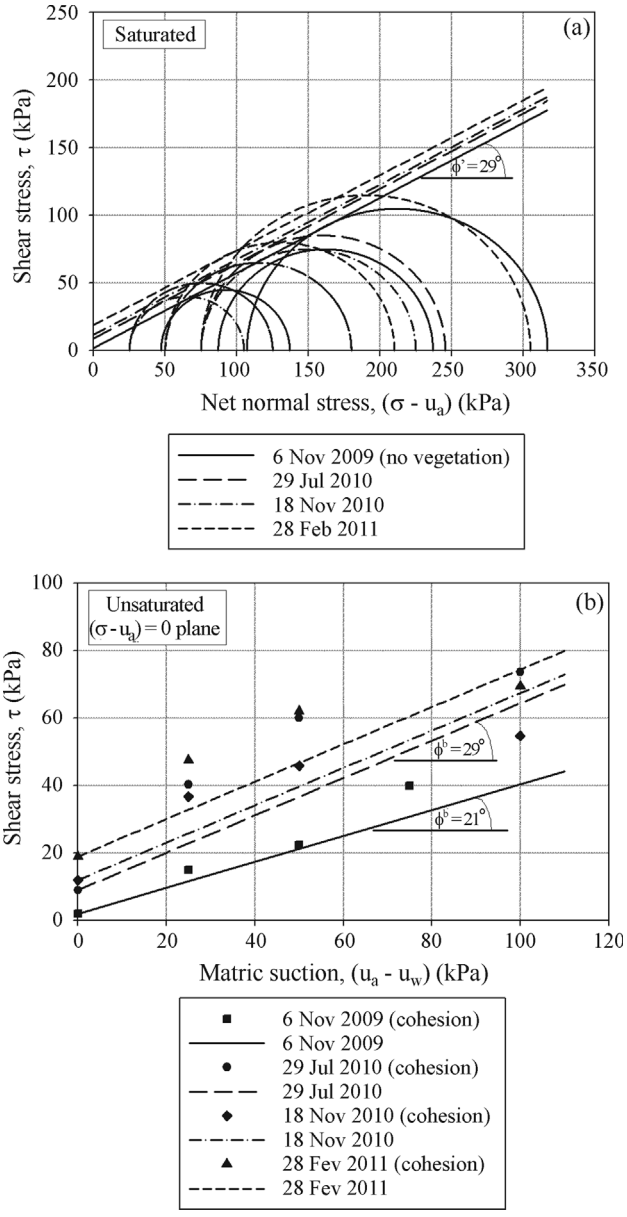

Figure 6 - Mohr-Coulomb failure envelopes of original soil and soil with Vetiver grass roots: (a) at zero matric suction, (b) at matric suctions greater than zero on $(\sigma - u_a) = 0$ plane.

shear strength envelope at zero matric suction (Figs. 5a and 6a) involves Mohr circles at failure and the envelope gives effective cohesion, *c'* and effective friction angle, ϕ'. The shear strength envelope at matric suctions greater than zero (Figs. 5b and 6b) was plotted on $(\sigma - u_a) = 0$ plane to obtain ϕ^b angle.

Comparison of shear strength parameters of the original soil (Layer 1) and the ones of the soils with Orange Jasmine roots and Vetiver grass roots in Figs. 5 and 6 and Table 7 indicates that the presence of Orange Jasmine and Vetiver grass roots increases the effective cohesion of soil. The ϕ^b angle of the soil with Orange Jasmine roots decreases from 21° to 18° and then increases to 27°, indicating that the ϕ^b angle of the soil with Orange Jasmine was relatively constant. The ϕ^b angle of the soil with Vetiver grass roots increases compare to the original soil.

5. Numerical Analyses

Numerical analyses were performed to investigate the effectiveness of CBS and vegetative slope covers in maintaining soil suction. Seepage and slope stability analyses were performed using the finite element software SEEP/W (GEO-SLOPE International Ltd. 2007a) and SLOPE/W (GEO-SLOPE International Ltd. 2007b), respectively.

Table 7 - Shear strength properties of the soils used in the study.

(a) Soils without vegetation.

Description	Symbol (unit)	Soils	
		Layer 1	Layer 2
Unit weight	γ (kN/m^3)	15.5	18.5
Effective cohesion	c' (kPa)	2	5
Effective friction angle	ϕ' (^{o})	29	37
	ϕ^b (^{o})	21	18

(b) Soils with Orange Jasmine roots.

Description	Symbol (unit)	Soil with Orange Jasmine root		
		29 Jul 2010	18 Nov 2010	28 Feb 2011
Unit weight	γ (kN/m^3)	16.3	19.8	20.2
Effective cohesion	c' (kPa)	15	21	23
Effective friction angle	ϕ' (^{o})	29	29	29
	ϕ^b (^{o})	18	18	27

(c) Soils with Vetiver grass roots.

Description	Symbol (unit)	Soil with Vetiver Grass root		
		29 Jul 2010	18 Nov 2010	28 Feb 2011
Unit weight	γ (kN/m^3)	16.5	19.5	20.4
Effective cohesion	c' (kPa)	9	12	19
Effective friction angle	ϕ' (^{o})	29	29	29
	ϕ^b (^{o})	29	29	29

(d) CBS.

Description	Symbol (unit)	Soils	
		Fine-grained layer	Coarse-grained layer (RCA)
Unit weight	γ (kN/m^3)	18	20
Effective cohesion	c' (kPa)	3.5	0
Effective friction angle	ϕ' (^{o})	44	49
	ϕ^b (^{o})	30	49

5.1 Slope geometries and boundary conditions

The boundary conditions (BC) for the numerical analyses are shown in Fig. 2. The boundaries were set as no flow boundaries at the bottom and as nodal flux, Q, equals to zero along the sides above water table. Constant head, H, was applied along the sides below water table. The actual rainfall was applied to the slope surface as a flux boundary, q. Ponding was not allowed to occur as water will run off the slope. Rainfalls at two time periods (the first time period represented the conditions prior to, during, and after the low intensity rainfall which occurred on 6 July 2010, named the period of low rainfall intensity while the second time period represented the conditions prior to, during, and after the high intensity rainfall which occurred on 25 November 2010, named the period of high rainfall intensity) were selected for the analyses (Figs. 7e and 8). Details of each of the rainfall events are shown in Fig. 8. The initial condition was based on the initial water table as measured using piezometers and pore-water pressure measurements from tensiometers (Figs. 7a to 7d).

Transient seepage analyses were performed for these two time periods. The results of numerical analyses were then compared with data obtained from field measurements. Analyses were performed for the original slope, slope with Orange Jasmine, slope with Vetiver grass, and slope with CBS. In the analyses for slope with Orange Jasmine and slope with Vetiver grass, SWCC and permeability function on 29 July 2010 were used for the seepage analysis of the period of low intensity rainfall whereas SWCC and permeability function on 18 November 2010 were used for the seepage analysis of the period of high intensity rainfall. The results of numerical analyses and data obtained from field measurements for each slope section were compared to evaluate the effectiveness of slope cover in maintaining soil suction in the slope especially during rainfall.

5.2 Seepage analyses

Results of the numerical analyses for the original slope, the slope with Orange Jasmine, the slope with Vetiver grass, and the slope with CBS within the period of low intensity rainfall are shown in Figs. 9 and 10. Results from field measurements are also shown together with results from numerical analyses. It is obvious from the field measurements as well as from the numerical analysis results (Figs. 9, 10, 11, and 12) that the presence of a sub layer with a lower saturated permeability, k_s, caused a higher increase in the pore-water pressure in this lower permeability layer as compared to the soil layer located above this layer. The numerical analyses showed good agreement with the data obtained from field measurements. Generally, the performances of the different slope covers in maintaining matric suction are essentially similar during the period of low intensity rainfall.

Results of the numerical analyses for the original slope, the slope with Orange Jasmine, the slope with Veti-

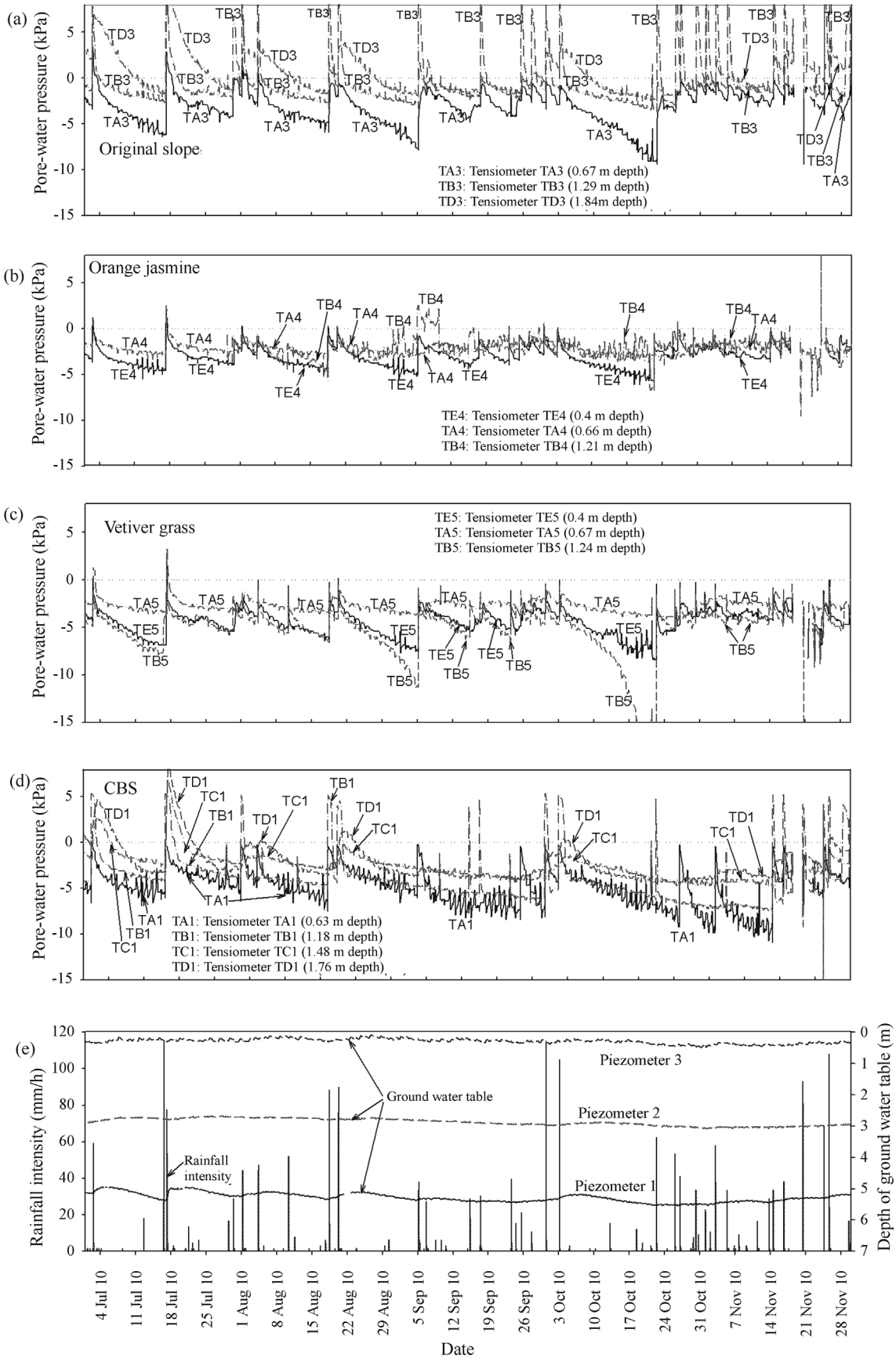

Figure 7 - Pore-water pressure, groundwater level, and daily rainfall *vs.* time.

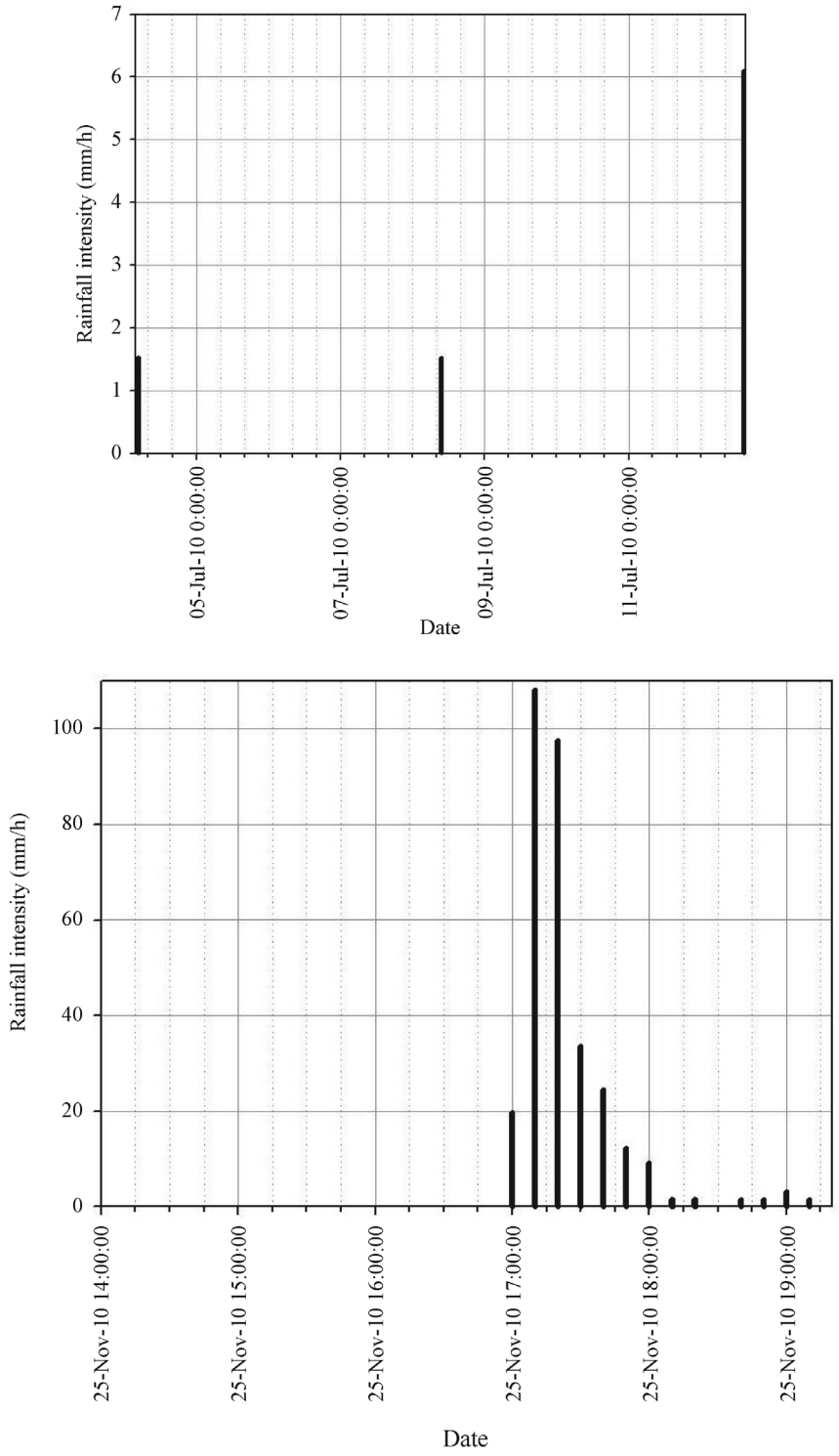

Figure 8 - Rainfall events used for the analyses. (a) Period of low intensity rainfall (prior to, during, and after 6 July 2010 rainfall event). (b) Period of high intensity rainfall (prior to, during, and after the 25 November 2010 rainfall event).

ver grass, and the slope with CBS at the period of high intensity rainfall are shown in Figs. 11 and 12. The performances of the different slope covers in maintaining matric suction are also essentially similar during the period of high intensity rainfall.

Both seepage analyses from the periods of low and high intensity rainfall showed that pore-water pressures in the slope sections with cover systems were always lower than those in the original slope without any cover system, illustrating the effective-

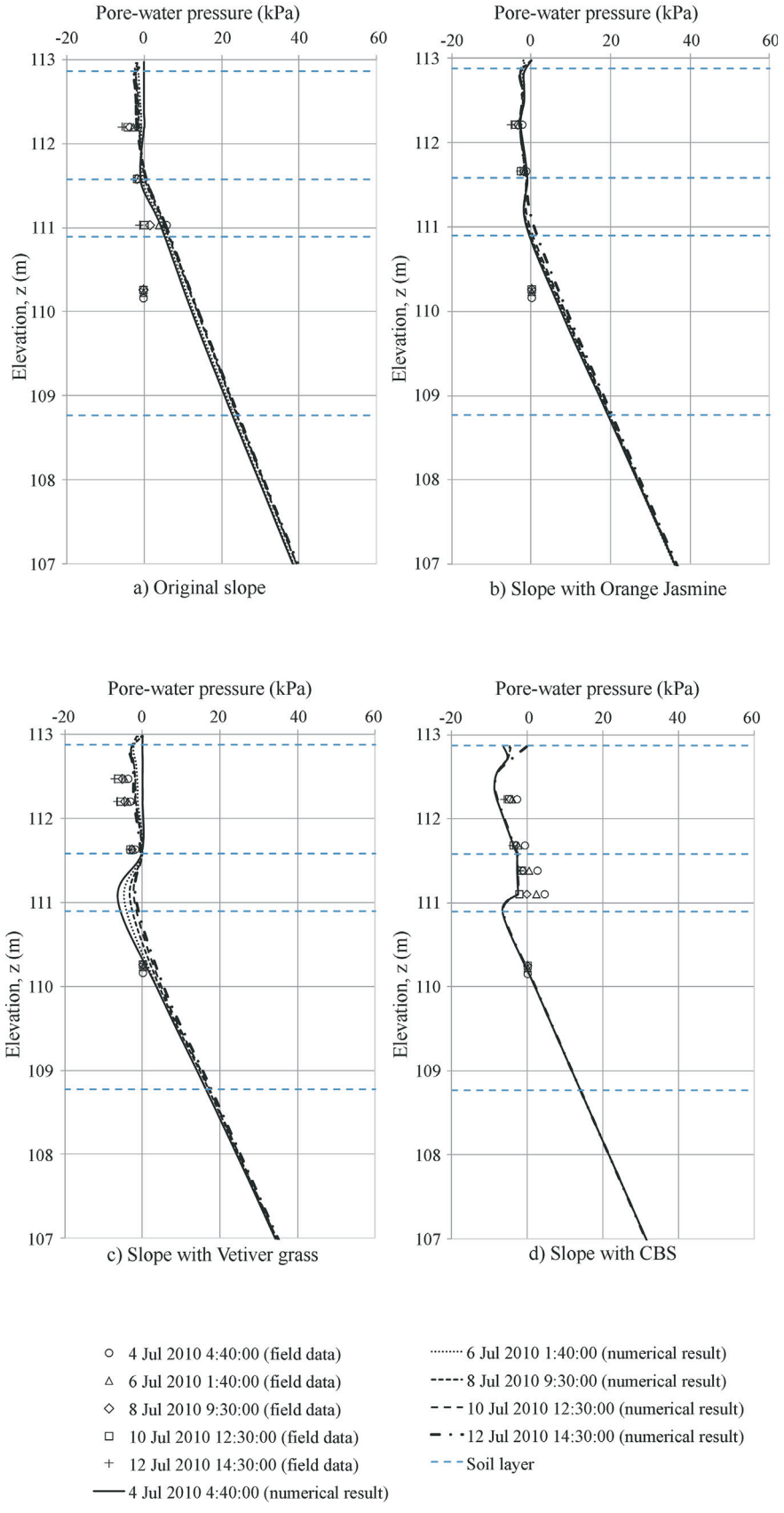

Figure 9 - Pore-water pressure profiles at each slope during the period of low intensity rainfall. (a) Original slope. (b) Slope with Orange Jasmine.(c) Slope with Vetiver grass. (d) Slope with CBS.

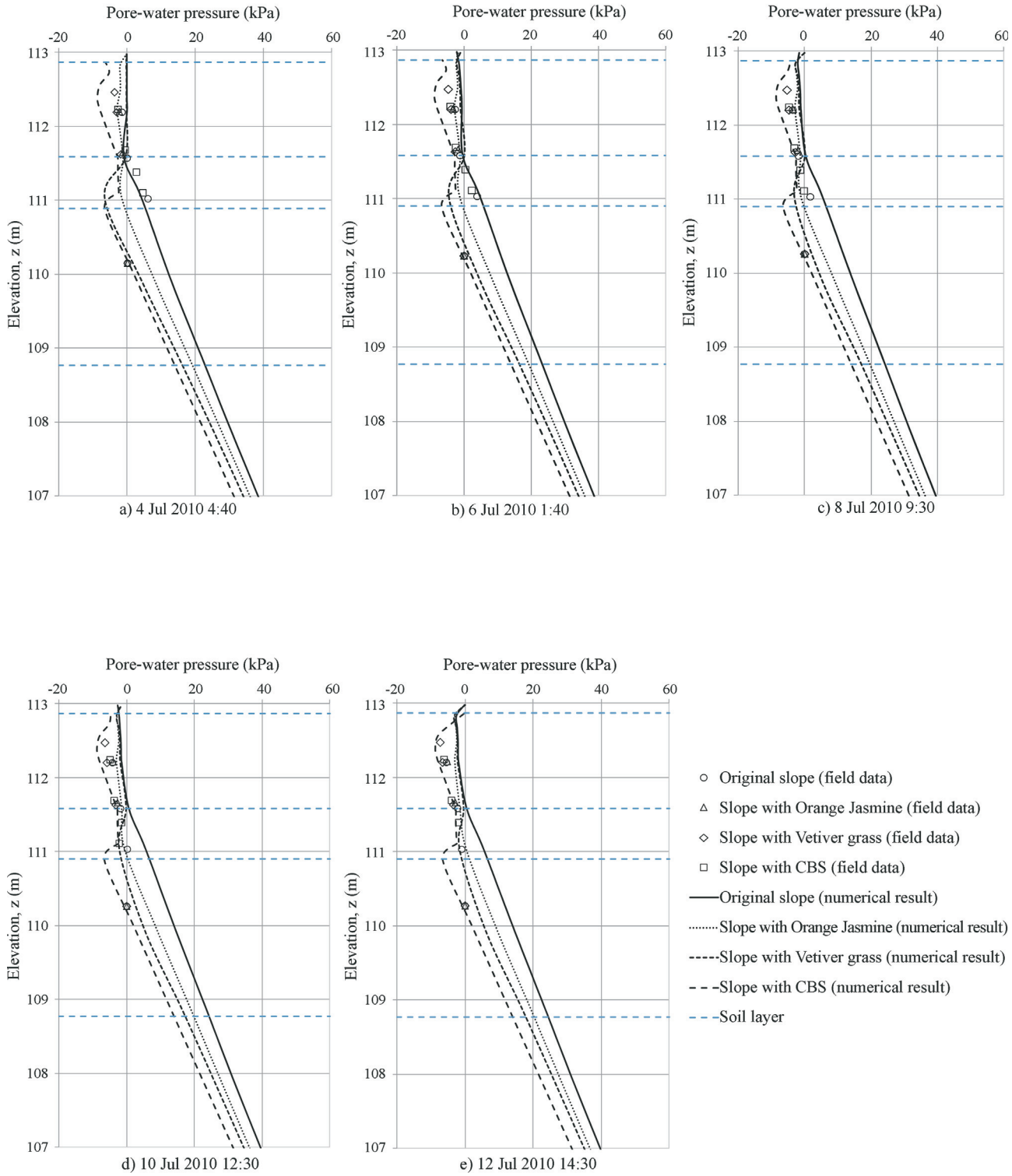

Figure 10 - Comparison of pore-water pressure profiles during the period of low intensity rainfall. (a) 4 Jul 2010 4:40. (b) 6 Jul 2010 1:40. (c) 8 Jul 2010 9:30. (d) 10 Jul 2010 12:30. (e) 12 Jul 2010 14:30.

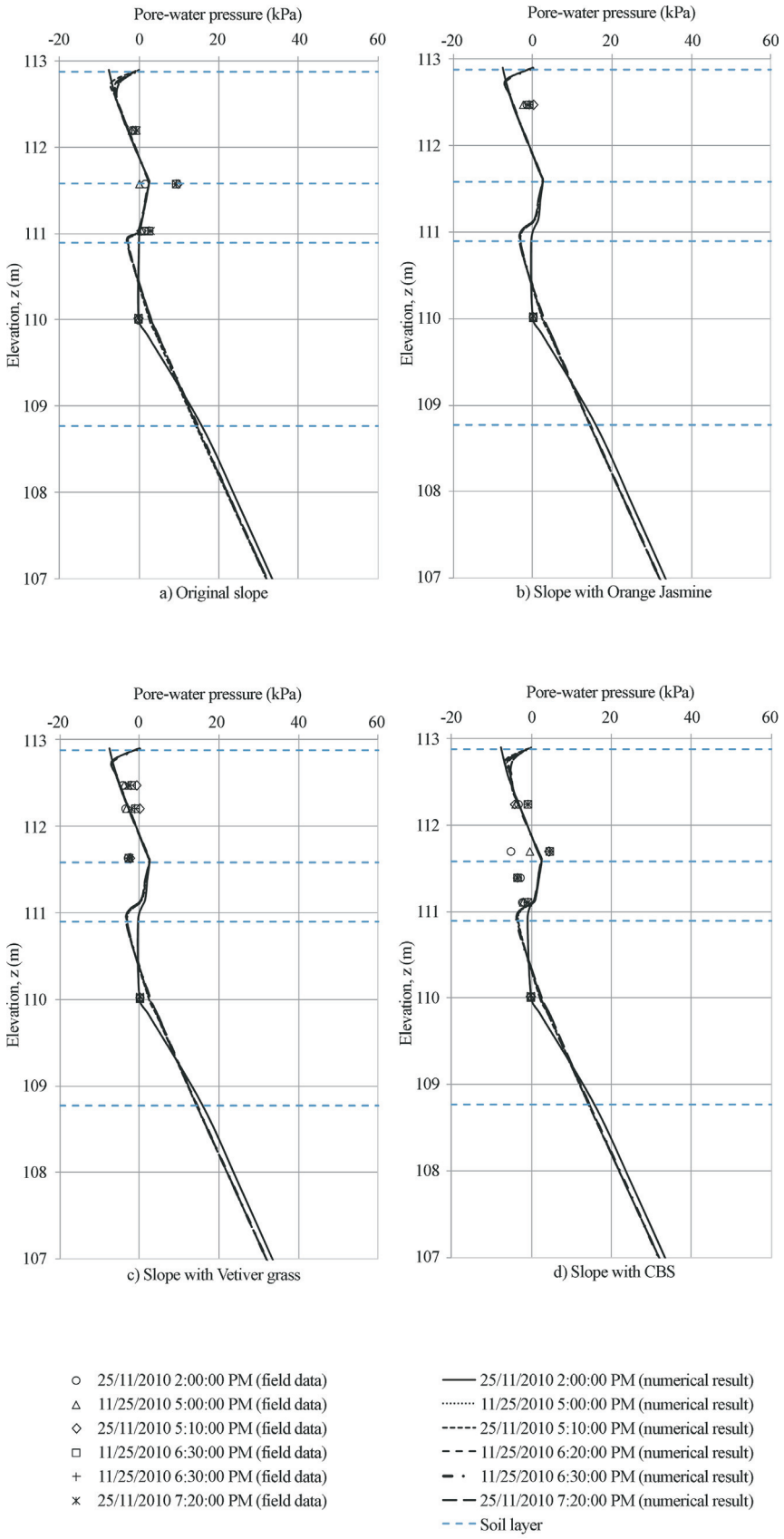

Figure 11 - Pore-water pressure profiles at each slope during the period of high intensity rainfall. (a) Original slope. (b) Slope with Orange Jasmine. (c) Slope with Vetiver grass. (d) Slope with CBS.

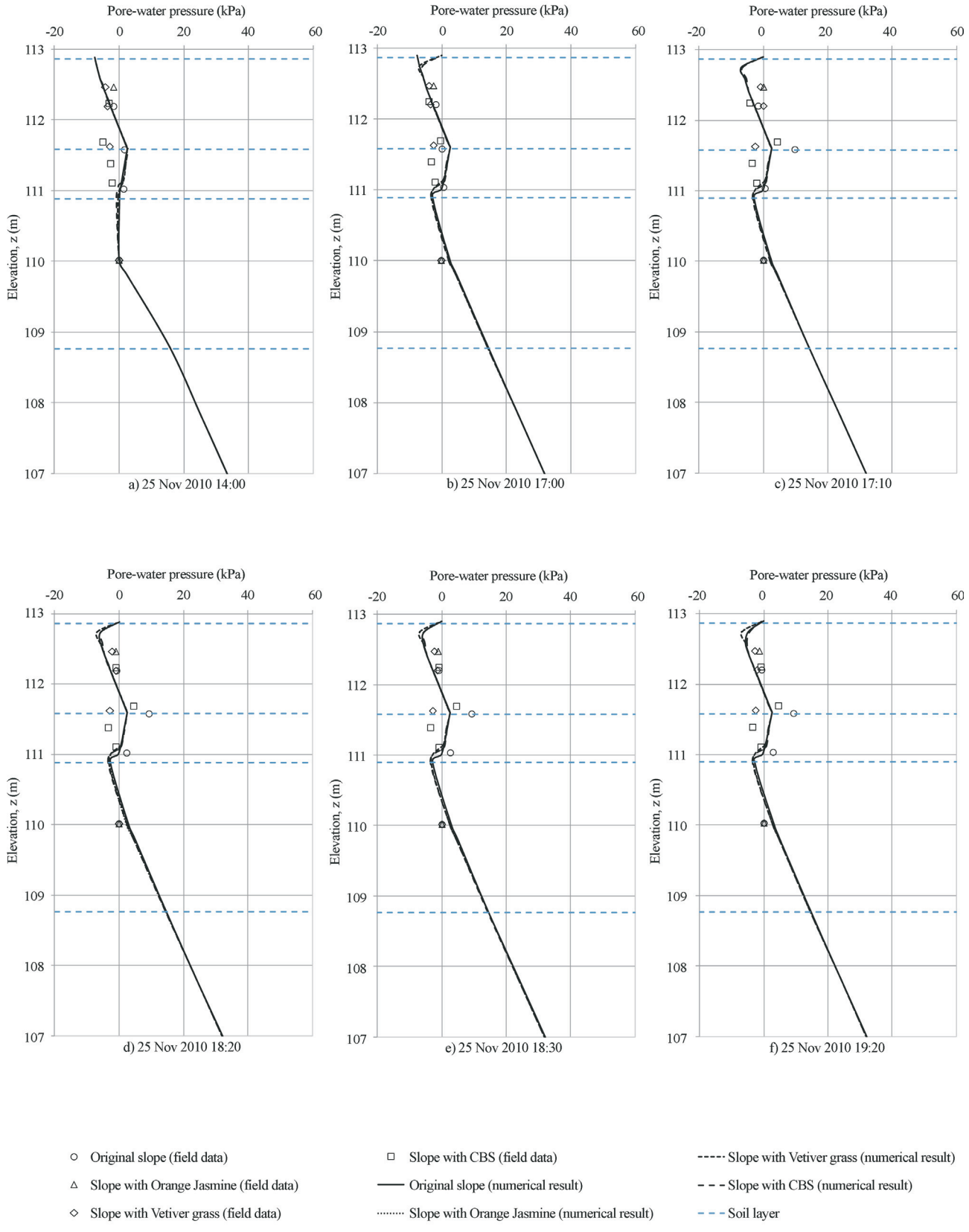

Figure 12 - Comparison of pore-water pressure profiles during the period of high intensity rainfall. (a) 25 Nov 2010 14:00. (b) 25 Nov 2010 17:00. (c) 25 Nov 2010 17:10. (d) 25 Nov 2010 18:20. (e) 25 Nov 2010 18:30. (f) 25 Nov 2010 19:20.

ness of cover system in maintaining soil suction in the slope during rainfall.

5.3 Slope stability analyses

Slope stability analyses were performed using Bishop simplified method by incorporating pore-water pressures at the periods of low and high intensity rainfall. Shear strength parameters used in the analyses are shown in Table 7. In the analyses for slope with Orange Jasmine and slope with Vetiver grass, the shear strengths on 29 July 2010 were used for the slope stability analyses of the period of low intensity rainfall whereas the shear strengths on 18 November 2010 were used for the slope stability analyses of the period of high intensity rainfall.

Variations of the factor of safety (FoS) of the different slopes during the period of low intensity rainfall are shown in Fig. 13. FoS of the slopes during the period of low intensity rainfall vary from 2.1 to 2.3. The small variation in FoS indicated that the performances of the different slope covers in maintaining matric suction in the slope were essentially similar.

Variations of FoS of the different slopes during the period of high intensity rainfall are shown in Fig. 14. FoS of the slopes during the period of high intensity rainfall vary from 2.0 to 2.1. The small variation in FoS indicated that the performances of the different slope covers in maintaining matric suction in the slope were essentially similar.

In addition to the above analyses, a stability analysis was performed using a maximum rainfall intensity of 533.2 mm/day that occurred continuously for 1 day based on a 25-year return period. This rainfall intensity is a maximum total amount of rainfall in a day of 533.2 mm that should be used in drainage system design in Singapore (PUB 2000). The effectiveness of the different slope covers experiencing this rainfall intensity was investigated through this analysis. The results are shown in Fig. 15.

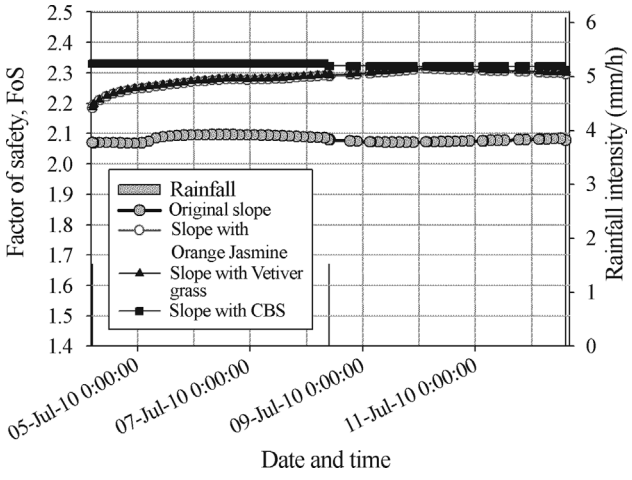

Figure 13 - Factor of safety variation during the period of the low intensity rainfall event on 6 July 2010.

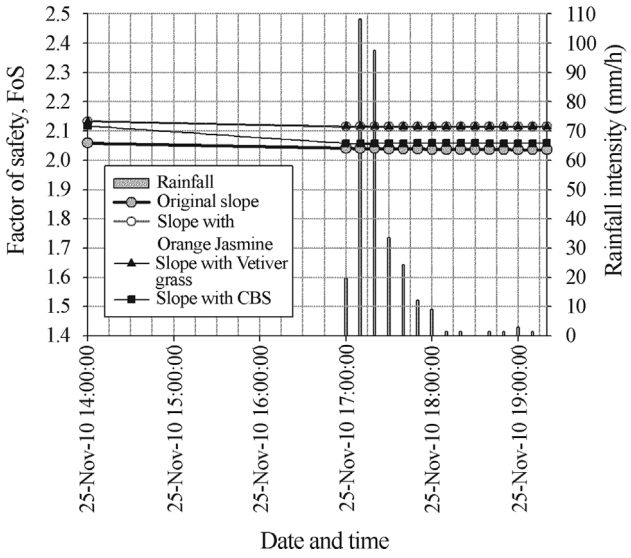

Figure 14 - Factor of safety variation during the period of the high intensity rainfall event on 25 November 2010.

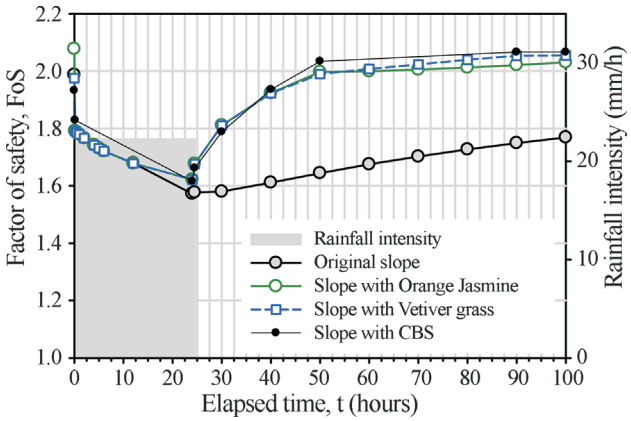

Figure 15 - Factor of safety variations during a high hypothetical rainfall intensity of 22.2 mm/h for 24 h.

The slopes had an initial FoS of around 2. After subjecting the slopes to the maximum daily rainfall, FoS of the slopes dropped to around 1.6. After the end of rainfall, FoS of the slopes with covers recovered faster than that of the original slope, indicating the effectiveness of the different cover systems in recovering FoS of the slopes after the maximum daily rainfall as compared to the original slope without cover. In addition, FoS of the slopes with slope covers were essentially similar throughout the study period.

6. Conclusions

Laboratory test results show that the presence of root increases shear strength of soils. The increase in shear strength is indicated by the increase in effective cohesion in both soils with Orange Jasmine roots and with Vetiver grass roots and by the increase in ϕ^b angle in the soil with

Vetiver grass roots. In addition to this, the presence of roots results in an increase in the saturated permeability and AEV of the soil.

Field monitoring results show that the slopes with slope covers can maintain negative pore-water pressures better than the original slope without cover. The amount of matric suction that can be maintained by the slope covers during the periods of low and high intensity rainfalls were similar for the slopes covered with Orange Jasmine, Vetiver grass, and CBS. As a result, FoS of slopes with the different covers were essentially similar during the low and high intensity rainfall periods. However, during the period of maximum intensity rainfall the slope covers resulted in a faster recovery of FoS of the slopes as compared to the original slope without the slope cover. In addition, FoS of the slopes with slope covers were essentially similar throughout the period of maximum intensity rainfall.

Acknowledgment

The work presented in this paper was supported by the Housing and Development Board and Nanyang Technological University, Singapore. Samwoh Pte Ltd provided the recycled concrete aggregate used in this study.

References

Brand, E.W. (1992). Slope instability in tropical areas. In: Proc. 6th International Symposium on Landslides, Christchurch, New Zealand, pp. 2031-2051.

Fredlund, D.G. & Rahardjo, H. (1993). Soil Mechanics for Unsaturated Soils. John Wiley & Sons Inc., New York, 517 p.

Fredlund, D.G. & Xing, A. (1994). Equations for the soil-water characteristic curve. Canadian Geotechnical Journal, 31(4):521-532.

Gasmo, J.M.; Rahardjo, H. & Leong, E.C. (2000). Infiltration effects on stability of a residual soil slope. Computers and Geotechnics, 26(2):145-165.

GEO-SLOPE International Pte. Ltd. (2007a). SEEP/W User's Guide for Slope Stability Analysis. Geoslope International Ltd., Calgary, Alberta, Canada, 307 p.

GEO-SLOPE International Pte. Ltd. (2007b). SLOPE/W User's Guide for Slope Stability Analysis. Geoslope International Ltd., Calgary, Alberta, Canada, 355 p.

Grimshaw, R.G. (1994). Vetiver grass-Its use for slope and structure stabilization under tropical and semitropical conditions. In: Vegetation and Slopes. Institution of Civil Engineers, London, pp. 26-35.

Khire, M.; Benson, C. & Bosscher, P. (2000). Capillary barriers: design variables and water balance. Journal of Geotechnical and Geoenvironmental Engineering, ASCE, 126(8):695-708.

Krisdani, H.; Rahardjo, H. & Leong, E.C. (2008). Measurement of geotextilewater characteristic curve using capillary rise principle. Geosynthetics International, 15(2):86-94.

Leong, E.C. & Rahardjo, H. (1997). A review on soil-water characteristic curve equations. ASCE Journal of Geotechnical and Geoenvironmental Engineering, 123(12):1106-1117.

Morel-Seytoux, H.J. (1994). Steady-state effectiveness of a capillary barrier on a sloping interface. In: Proc. 14th Hydrology Days Conference, Fort Collins, pp. 5-8.

Morel-Seytoux, H.J. (1993). Dynamic perspective on the capillary barrier effect at the interface of an upper fine layer with a lower coarse layer. In: Proc. of Engineering Hydrology, San Francisco, pp. 467-472.

Morris, C.E. & Stormont, J.C. (1997a). Capillary barriers and subtitle D covers: Estimating equivalency. Journal of Environmental Engineering, ASCE, 123(1):3-10.

Morris, C.E. & Stormont, J.C. (1997b). Closure to "Capillary barriers and subtitle D covers: estimating equivalency" by Carl E. Morris and John C. Stormont. Journal of Environmental Engineering, ASCE, 123(1):3-10.

National Research Council (1993). Vetiver Grass: A Thin Green Line Against Erosion. National Academy Press, Washington DC, 188 p.

Pham, H.; Fredlund, D.G. & Barbour, S.L. (2005). A study of hysteresis models for soil-water characteristic curves. Canadian Geotechnical Journal, 42(6):1548-1568.

Pitts, J. (1985). An Investigation of Slope Stability on the NTU Campus, Singapore. Applied Research Project RPI/83. Nanyang Technological Institute, Singapore.

PUB (2000). Code of Practice on Surface Water Drainage. Public Utilities Board, Singapore, 63 pp.

Ross, B. (1990). The diversion capacity of capillary barriers. Water Resources Research, 26(10):2625-2629.

Steenhuis, T.S.; Parlange, J.-Y. & Kung, K.-J. (1991). Comment on "The Diversion Capacity of Capillary Barriers" by Benjamin Ross. Water Resources Research, 27(8):2155-2156.

Stormont, J.C. (1996). The effectiveness of two capillary barriers on a 10% slope. Geotechnical and Geological Engineering, 14(4):243-267.

Styczen, M.E. & Morgan, R.P.C. (1995). Engineering properties of vegetation. In: R.P.C. Morgan and R.J. Rickson (eds) Slope Stabilization and Erosion Control. E & FN Spon, London, pp. 5-58.

Tami, D.; Rahardjo, H.; Leong, E.C. & Fredlund, D.G. (2004a). A physical model for sloping capillary barriers. Geotechnical Testing Journal, 27(2):173-183.

Tami, D.; Rahardjo, H.; Leong, E.-C. & Fredlund, D.G. (2004b). Design and laboratory verification of a physical model of sloping capillary barrier. Canadian Geotechnical Journal, 41(5):814-830.

Tan, S.B.; Tan, S.L.; Lim, T.L. & Yang, K.S. (1987). Landslides problems and their control in Singapore. In: Proc. 9th Southeast Asian Geotechnical Conference, Bangkok, Thailand, v. 1, pp. 25-36.

TenCate (2011). TenCate Polyfelt TS Nonwoven Geotextiles. TenCate Geosynthetics Asia Sdn. Bhd. Selangor Darul Ehsan, Malaysia, 8 pp.

Truoung, P. & Gawander, J.S. (1996). Back from the future: do's and don'ts after 50 years of Vetiver utilisation in Fiji. Proc. First International Conference on Vetiver. Office of the Royal Development Projects Board, Bangkok, pp. 12-17.

Tsaparas, I.; Rahardjo, H.; Toll, D.G. & Leong, E.C. (2002). Controlling parameters for rainfall-induced landslides. Computers and Geotechnics, 29(1):1-27.

World Bank (1995). Vetiver Grass for Soil and Water Conservation. Technical Paper No. 273. RG Grimshaw (ed), Washington DC, 281 p.

Yang, H.; Rahardjo, H.; Leong, E.C. & Fredlund, D.G. (2004b). A study of infiltration on three sand capillary barriers. Canadian Geotechnical Journal, 41(4):629-643.